

LONDON, METEOROLOGICAL OFFICE.

Met.O.15 Internal Report No.50.

A case study of the microphysics and dynamics of a stratocumulus layer with horizontal roll vortices present. By TURTON, J.D.

London, Met. Off., Met.O.15 Intern. Rep. No. 50, 1983, 31cm. Pp. [ii] + 27, 17 pls. 33 Refs. Abs. p. [i].

An unofficial document - not to be quoted in print.

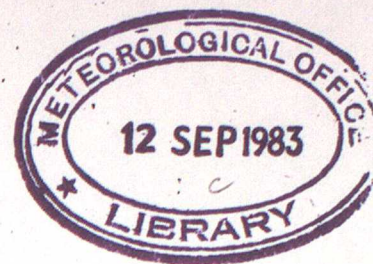
FG2

National Meteorological Library
and Archive

Archive copy - reference only

METEOROLOGICAL OFFICE

London Road, Bracknell, Berks.



141250

MET.O.15 INTERNAL REPORT

No 50

A Case Study of the Microphysics
and Dynamics of a Stratocumulus
Layer with Horizontal Roll
Vortices Present

By

J D Turton

August 1983

Cloud Physics Branch (Met.O.15)

SUMMARY

Observations of stratocumulus from an instrumented aircraft are presented and discussed. Detailed microphysical measurements (drop-size distributions, concentrations and liquid water contents) were made which exhibited periodic fluctuations. Dynamical measurements and visual observations suggested the presence of horizontal roll vortices in the cloudy boundary layer. The dynamical structure of the rolls was observed to modulate the microphysical structure of the cloud. This was due primarily to radiative cooling of droplets (causing droplet growth) carried close to cloud top by the roll circulation. A simple Lagrangian model with a specified parcel trajectory representative of the roll circulation is able to produce droplet population variations similar to those observed. The observations show the crucial effect of the cloud dynamics on the microphysical structure of the cloud layer. During the flight droplets of radius greater than $20\mu\text{m}$ were found which were presumed to have formed by coalescence and this is discussed. Gravity waves above the cloud top inversion were also observed and these are also discussed.

1. INTRODUCTION

Measurements of stratocumulus are relatively sparse, although there have been many attempts to model stratocumulus. James (1959) made one of the first major aircraft studies of stratocumulus and his and other early work was reviewed by Cornford (1966). Paltridge (1974) made radiometric measurements and related them to the microphysics, similar measurements were later made by Platt (1976). Recent observations of stratocumulus using an aircraft have been described by Coulman (1978) who investigated convective motions in the cloud and by Slingo et al. (1982b) who discussed radiative and microphysical measurements made during the JASIN experiment. A field study of nocturnal stratocumulus at Cardington, UK, using a tethered balloon has been carried out and the results have been described by Roach et al. (1982), Caughey et al. (1982a), Slingo et al. (1982a) and Caughey et al. (1982b). Observational studies of horizontal roll vortices have been described by Konrad (1968), Kuettner (1971) and more recently by LeMone (1973, 1976). Numerical studies of rolls have also been made, Kuettner (1971) and Mason and Sykes (1980, 1982) being two examples.

The data presented in this study is particularly interesting because the detailed microphysical measurements obtained exhibit a periodic fluctuation in space which it is suggested is a result of the dynamical structure of the cloudy boundary layer. Details of the flight, whose main objective was to study the transport of air pollutants are given by Fisher (1981). During sampling off the east coast of the UK in the North Sea on 28 January 1981 a series of level runs and profiles were made in and above an extensive layer of stratocumulus. Flight observers reported that the layer of stratocumulus exhibited a periodic structure. Photographs taken from the aircraft while above the cloud layer show regularly spaced bands of thicker cloud, which it is suggested are due to rolls. Unfortunately since the photographs were taken in the late afternoon near sunset their quality is too poor to allow reproduction here. Rolls of cloud or bands of thicker cloud along the wind have often been observed and they result from

convection within a shallow layer in the presence of wind shear. The data obtained during this flight contained information on both the dynamical and microphysical structure of the cloud layer. Detailed microphysical and dynamical measurements of stratocumulus exhibiting rolls have not previously been available and so the data presented are of interest to cloud physics and boundary layer studies.

2. INSTRUMENTATION

The instrumentation of the Meteorological Research Flight C130 aircraft has been recently described by Crabtree and Marsh (1981). The turbulence instrumentation has been fully described by Nicholls (1978). The three wind components were measured by a combination of wind vanes, a high quality pitot-static system and an inertial platform. Drifts of the inertial platform were removed by reference to a doppler radar and radar altimeter. The horizontal and vertical winds are accurate to about 0.4 ms^{-1} and 0.1 ms^{-1} with a resolution of about 0.07 ms^{-1} and 0.03 ms^{-1} respectively. The wind measurements were recorded at 40 Hz. Air temperature was measured using a platinum resistance thermometer to an accuracy of 0.2 deg C with a resolution of 0.006 deg C . Temperatures were sampled at 20 Hz and both temperatures and winds were recorded in the aircraft at 20 Hz giving a spatial resolution of about 5 m at typical airspeeds of 100 ms^{-1} . Liquid water content was measured using a Johnson-Williams hot wire instrument (Johnson 1979, Ouldrige 1982b). The device measures liquid water contents up to 3 gm^{-3} but underestimates the liquid water when droplets larger than $30 \mu\text{m}$ are present. Microphysical measurements were made with an Axially Scattering Spectrometer Probe (ASSP), (see Knollenberg 1976) and a Particle Measuring Systems two dimensional probe (PMS 2D), (see Knollenberg 1970). The ASSP counts and sizes droplets in the size range 2 to $24 \mu\text{m}$ radius and droplet spectra can be produced for 1 s samples (i.e. 100 m spatial resolution). The ASSP used in this study has been considerably modified

(Ryder 1976, Roach 1977) but although it gives accurate dropsizes distributions, absolute concentrations and liquid water contents are doubtful due to the uncertainty in the sampling volume. For this reason concentrations from the ASSP were scaled to give liquid water contents which agreed with those obtained from the Johnson-Williams which has a better absolute accuracy. All of the liquid water content measurements presented in this paper are from the Johnson-Williams. Larger cloud droplets were measured using the PMS 2D "cloud" probe which counts and sizes particles in the range $25\text{--}800\text{ }\mu\text{m}$. The PMS 2D "precipitation" probe which counts and sizes particles in the range $200\text{ }\mu\text{m}$ - 6.4 mm was found to have been faulty during this flight. Details of the PMS 2D probes used in this study are given by Ouldridge (1982a). Droplet spectra from the PMS 2D "cloud" probe were integrated over 10 s intervals in this study to allow integrated spectra from the PMS 2D and the ASSP to be combined. Larger cloud droplets as measured by the PMS 2D were only encountered during profile 2 and are discussed later.

3. SYNOPTIC SITUATION

Fig. 1 shows the synoptic situation at 1200 GMT over western Europe. An anticyclone was centred over Germany which maintained a south west gradient wind of 20-25 knots across the east coast of the UK. The solid line shows the positions of the aircraft runs analysed in this study, these runs were made across the direction of the gradient wind. Fig. 2 is a satellite picture at visible wavelengths taken at 0923 by NOAA-6, the extent of the stratocumulus over Britain and the North Sea is clear. In the area of study the cloud appears solid with no obvious structure. Over northern England and Scotland waves are apparent in the cloud layer. There was no evidence of any upper cloud above this stratocumulus layer from the infra-red satellite pictures nor was any high level cloud observed in the area by aircraft observers.

4. CLOUD AND BOUNDARY LAYER STRUCTURE

From Fig. 1 it can be seen that the aircraft runs were made acrosswind. Level runs were made at different heights in and above the cloud, and two profiles were made through the cloud. Profile and horizontal run data have been used to construct a two dimensional cross-section of the cloud layer since most of the level runs were through the same area of cloud. Satellite pictures show little change in the cloud layer during the day so advection and development effects have been ignored. Fig. 3 shows the cross-section obtained. As measurements at cloud base were limited, the cloud base height was estimated by calculating the saturated adiabatic ascent necessary to give the maximum values of liquid water obtained during the lower runs in cloud. The assumptions of the technique are consistent with liquid water profiles measured in stratocumulus at Cardington (Slingo et al. 1982a). The cloud top is capped by a marked temperature inversion, a common feature of stratocumulus, also observed in the Cardington studies (Roach et al. 1982, Slingo et al. 1982a). The profile data indicates the variation in cloud top height as the inversion level changes.

a. Microphysical structure of the cloud layer

i. Aircraft profiles

As mentioned previously two profiles were made through the cloud layer and the positions of these are shown by Fig. 3. Figs. 4(a) - 4(d) show the variations of temperature, liquid water content (from the Johnson-Williams), droplet concentration (corrected against the Johnson-Williams) and droplet mean volume radius (as measured by the ASSP) with height obtained during profile 2 near $53^{\circ}20'N$. Cloud top is identified at a height of about 520 m by a temperature inversion of 3.5 deg C over 35 m. The cloud base is at about 150 m. The liquid water content increases with height at a rate which varies between half of the adiabatic rate and the adiabatic rate. The departure of the cloud

water content from the adiabatic value is probably due to entrainment of dry air from above the inversion. The close agreement between the change of water content with height and the adiabatic rate in the lowest 70 m of the cloud is additional justification for the method of estimating the cloud base. In the upper half of the cloud the increase in liquid water content is associated with an increase in droplet radius (Fig. 4d). Within 100 m of cloud top a decrease in droplet concentration with height is observed. These observations are consistent with the hypothesis of inhomogeneous mixing as described by Latham and Reed (1977). Entrainment of dry air in an inhomogeneous way has the effect of reducing the droplet concentration but does not affect the distribution of droplet sizes. On the other hand if the mixing is homogeneous then the peak of the droplet spectrum is shifted towards lower sizes as the entire population of drops evaporate but the concentration is largely unaffected. In the lower half of the cloud the droplet concentration increases with height from the cloud base.

The structure of the droplet field is shown in Fig. 5, this profile is constructed using dropsize distributions and concentrations from the ASSP (corrected) and PMS 2D from data obtained during profile 2. The ASSP data have been meaned over 10 s periods synchronized with the PMS 2D data to provide the necessary distributions, giving a vertical resolution of at least 20 m. For droplets of radii detected by both instruments the (corrected) ASSP concentrations were used since the PMS 2D is less accurate in counting droplets in the size range 13-24 μm radius. Throughout the depth of the cloud layer droplets of up to 20 μm radius are present, the existence of drops of about 20 μm radius is common in stratocumulus. Frith (1951) found droplets of this size in concentrations of at least 100 litre⁻¹ (10^{-1} cm^{-3}) in thin layers of stratocumulus where the mean volume radius was around 6 μm . The data presented here is consistent with the above measurements of Frith (1951). These larger drops are probably droplets that have had a longer lifetime within the cloud,

with any further growth in droplet size likely to be due to coalescence. In the lower half of the cloud the total droplet concentration decreases towards cloud base but the concentration of large drops of radius greater than $40\text{ }\mu\text{m}$ increases towards cloud base. The maximum dropsizes observed also increases from around $20\text{ }\mu\text{m}$ just above the middle of the cloud layer to about $100\text{ }\mu\text{m}$ at cloud base. Below the cloud base these larger droplets still exist and a thin patch of cloud is present at about 75 m above the sea surface, this patch of cloud coincides with a low level inversion. Stewart (1964) observed precipitation from warm layer clouds with depths as shallow as 0.4 km, similar to that in this study. The amount of liquid water contained in the large droplets is very small, due to the low concentrations of such droplets. The liquid water spectrum obtained at 200 m (near to cloud base) shows no significant secondary peak at large dropsizes.

Figs. 6(a) - 6(d) show data obtained during profile 3 near $53^{\circ}55'\text{N}$. The profile was started at 150 m above the sea surface which was within the cloud at this location. Cloud top was at about 400 m and coincided with a temperature inversion of 6.0 deg C over 55 m. The liquid water content increases with height above cloud base at nearly the adiabatic rate indicating little or no entrainment in this area. Cloud base was estimated to be at about 40 m height by extrapolation of the liquid water content data. The droplet mean volume radius increases only slowly with height, whereas the droplet concentration (which shows considerable scatter) increases with height. It is possible that all of the cloud condensation nuclei are not activated at cloud base and the supersaturation increases with height through the cloud so that more nuclei are activated. If this interpretation is correct it is to be contrasted with the usual situation in convective cloud in which the peak supersaturation is near to cloud base and the droplet concentration is insensitive to height above cloud base. The scatter in concentration is probably due to inhomogeneities in the boundary layer, the consequences of which are discussed in section 5. It is

noticeable that the droplet concentrations measured near 53°55'N are higher than those around 53°20'N, this is possibly due to a higher background nuclei concentration due to some anthropogenic source.

b. Dynamical structure of the boundary layer.

i. Aircraft observations

Fig. 3 shows the cloud cross-section and the positions of the level runs in and above the cloud. To reduce the data to a manageable quantity only segments of each run were studied. Each segment was of up to five minutes length (i.e. up to 30 km in horizontal extent) and the segments analysed were located around 53°35'N and 53°55'N. Time series of the measured vertical velocity component along the legs in cloud, which were orientated across the direction of the wind indicate well defined vertical velocity fluctuations of order $\pm 1 \text{ ms}^{-1}$. These fluctuations had a period of typically 20 s, corresponding to a length scale of approximately 2 km. Fig. 7(a) shows an example of these fluctuations measured in the cloud. Around 53°35'N the scale of the fluctuations is typically 1.5 km and around 53°55'N is typically 2.0 km. At about 80 m above the cloud top (at 53°55'N) a variation is still observed on this scale, see Fig. 7(b). This structure above the cloud shows little evidence of any smaller scale variation suggesting that turbulence is not present. The small scale structure seen within the cloud suggests the existence of turbulence. These suggestions are supported by spectral analyses (using a fast Fourier transform technique) of 20 Hz data. Each spectrum was computed from 8192 data points, so that the sample extends over 40 km. Data were detrended before the spectra were computed. The power spectra of data from within and above the cloud layer are significantly different. Figs. 8(b) and 8(c) show vertical velocity spectra obtained in the cloud layer at 295 m and 150 m height above the sea surface respectively. Fig. 8(a) shows the vertical velocity spectrum obtained above the cloudy boundary layer. In cloud the spectra exhibit

a well defined inertial subrange slope of approximately $-2/3$. Such a slope is present in spectra obtained throughout the depth of the cloud, suggesting the existence of turbulence. In contrast the spectrum obtained above the cloud layer shows a much more rapid fall off of energy at high frequencies suggesting that the velocity fluctuations may be due to gravity waves excited by the cloud layer motions. This is shown by Fig. 8(a) which is a vertical velocity spectrum obtained above the cloudy boundary layer, a well defined peak at 0.045 Hz corresponding to a length scale of 2.2 km is present. It is believed that this peak is due to internal gravity waves caused by the convective motions (rolls) within the boundary layer which cause perturbations of the capping inversion. This spectrum (Fig. 8(a)) has a slope of approximately $-5/3$ and is consistent with previous spectra of gravity waves which have produced slopes of $-5/3$ (Axford 1971) and $-6/3$ (Caughey and Palmer 1979). The corresponding spectra of horizontal velocity components (u and v) also show this different structure in and above the cloudy boundary layer. Corresponding spectra of temperature (T) also suggest this behaviour, but the time series contain longer period changes which complicate the analysis of the spectra. The boundary layer spectra of Figs. 8(b) and 8(c) are further discussed in the following section.

ii. Horizontal roll vortices

As previously mentioned rolls of cloud or a cloud structure with thicker bands orientated along the wind direction have often been observed. They are a result of horizontal roll vortices in the boundary layer. Rolls are an important mechanism for the vertical transfer of heat, momentum and water vapour in the boundary layer. Previous studies of convective rolls in clear air have been described by Konrad (1968), while Kuettner (1971) and LeMone (1973, 1976) reported observations of cloud streets. These observations can be compared with those in this study as the dynamical structure are similar, the differences being due to the presence of cloud. Kuettner (1971) suggests that cloud street

spacing varies from 2 km to 8 km and the cloud bands may be of up to 500 km in length, that street spacing is between 2 and 4 times the boundary layer depth with the streets orientated about 15° to the left of the geostrophic wind. Measurements by LeMone (1973) agreed with his observations. She found street spacing varied between 1 km and 8 km, and decreased with vertical instability. In her studies the ratio of roll horizontal wavelength to roll depth were variable but typically were in the range 2 to 4, the rolls were generally orientated $10-20^\circ$ to the left of the wind at the base of the inversion. LeMone found that rolls consistently occurred in moderately strong winds over uniform terrain and in slightly unstable conditions.

In this study the scale of the vertical velocity fluctuations is about 1.5 km at $53^\circ 35'N$, about 3 times the local boundary layer depth, while at $53^\circ 55'N$ the scale is about 2.0 km, about 5 times the local boundary layer depth. These ratios fall within those observed by LeMone (1973) for horizontal roll vortices. The cloud top structure observed from the photographic records was at an angle of approximately 80° to the flight path which was across the wind, is consistent with the orientations observed in previous studies. Unfortunately the quality of photographs of the cloud bandedness are too poor to allow reproduction in this paper.

The fundamental problem with the data available is that it is difficult to extract positive evidence for the existence of the rolls. Despite the poor quality photographic evidence for the rolls and individual observations by aircraft observers of them, it has not proved possible to independently show the existence of the rolls from the recorded data. An attempt was made to find evidence of the coherent structure of updraughts which ought to occur in a roll circulation. Although some suggestion of coherence was found the results were inconclusive. This is due to two reasons, (i) it was not possible to identify the aircraft position at a given time to a sufficient accuracy (i.e. to within about 1 km) and (ii) the vertical velocity time series and spectra in the

cloud show a continuous spectrum of updraughts on scales up to the predominant roll scale, making identification of definite roll updraughts difficult. Nonetheless despite the absence of independent evidence for the rolls there is no doubt that they did exist on this occasion. Some indirect evidence for the rolls exists in the presence of the gravity waves in the stable region above the boundary layer. It is suggested that the gravity waves are caused by the boundary layer motions (rolls) perturbing the inversion. Numerical studies of convective rolls by Mason and Sykes (1982) have suggested that gravity waves may occur, although gravity wave generation (in their model) was sensitive to most parameters, particularly roll orientation.

LeMone (1973) determined that bouyancy provides the main driving force for the rolls, even in near neutral conditions and that the windshear is important in providing the mechanism to organise convection into rolls. Fig. 9 shows the winds observed during profile 2. The windspeed increases and the wind veers below the cloud. In the cloud layer the wind has little shear, but at the inversion capping the boundary layer there is strong shear as the wind decreases with increasing height. Similar shear was also seen at the inversion during profile 3. The wind profiles observed at Cardington (Roach et al. 1982) and during JASIN (Slingo et al. 1982b) showed little shear through the inversion and in their analyses no roll circulations were apparent.

The later work of LeMone (1976) on cloud streets reported spectra which indicated a partitioning of the energy between the large scale rolls which were on a scale of 2.1 km and the smaller scale turbulence on scales up to 210 m. The existence of such a spectral window suggests that there is little energy exchange between the two scales. This has allowed Mason and Sykes (1980, 1982) to model motion on the scales separately. LeMone found that the roll energy accounted for a significant part of the total low frequency energy. She suggested that the additional energy in the total low frequency energy reflected the presence of some rolls with stronger circulation, kilometer scale cells

superimposed on the rolls or other irregularities, referring to these three categories as "kilometer scale turbulence". The rolls observed in the present study differ from those observed by LeMone in that the spectra (examples of which are shown in Figs. 8(b) and 8(c)) suggest the existence of energy on scales right up to the roll scale, with no evidence of a spectral gap. This spectral structure is confirmed by spectra of shorter periods of data containing fewer rolls. The spectra suggest the existence of significant "kilometer scale turbulence". The absence of a spectral gap in this study implies that energy travels from the rolls into smaller scale turbulence. The spectra (Figs. 8(b) and 8(c)) exhibit significant peaks near 0.05 Hz (2 km) which are probably due to rolls, although the roll spectral signatures are less well defined than those shown by LeMone (1976). The spectra (Figs. 8(a), 8(b) and 8(c)) show another interesting feature in that energy on a much larger scale of approximately 0.01 Hz (10 km) is also present. Energy on this scale is present above the cloud (Fig. 8(a)) and in the cloud at 295 m (Fig. 8(b)) and at 150 m (Fig. 8(c)). At 150 m the energy on this scale is attenuated but still shows a spectral peak. An enlarged version of the satellite image of Fig. 2 shows the presence of large scale gravity waves over northern England and Scotland, suggesting that such gravity waves may be responsible for the energy on this scale. As mentioned previously the spectra show significant peaks which are probably due to rolls, the frequencies of these peaks can be related to a characteristic wavelength $(\lambda_m)_w$ for the vertical velocity fluctuations. Fig. 10 shows $(\lambda_m)_w$ plotted against height for the rolls in this region (around 53°55'N) and for the roll generated gravity waves above the boundary layer. A typical $(\lambda_m)_w$ of about 2 km is found with some suggestion of a reduction in scale nearer to the sea surface.

5. MICROPHYSICAL AND DYNAMICAL INTERACTION IN THE CLOUD

a. Aircraft observations

As previously mentioned the microphysics and dynamics of the cloud layer are related. The dominant scale of the vertical velocity fluctuations (~ 2 km) is also seen in the microphysics during the level runs. Figs. 11(a), 11(b) and 11(c) show that regions of high droplet concentration correlate strongly to those with a small mean volume radius (and low spectrum dispersion). The regions of high concentrations are correlated with the updraughts in the cloud layer. The Figs. show this behaviour at 175 m above the sea surface (in the bottom half of the cloud) at $53^{\circ}55'$ N, but such behaviour is observed through the depth of the cloud. The correlation of the microphysics to the dynamics appears to vary with height through the cloud becoming weaker towards cloud top. This is probably due to entrainment at cloud top which affects the droplet population close to the entrainment interface. The correlation at $53^{\circ}55'$ N is less height dependent than that at $53^{\circ}35'$ N and this gives support to this idea, since the inversion was stronger and mixing was less evident from the liquid water profile at $53^{\circ}55'$ N. The relationship between the microphysics and the dynamics is more closely examined in Figs. 12(a), 12(b) and 12(c) which illustrate the variations during a 50 s period during run 4 at 175 m (around $53^{\circ}55'$ N). The shorter period shown by Fig. 12 is included in the longer period shown by Fig. 11. Figs. 12(a) and 12(b) show time histories of droplet concentration and vertical velocity fluctuation and 12(c) shows contours of droplet concentration for dropsize (given by the ASSP channel ranges as in Table 1) calculated from ASSP spectra produced every second. In the major updraughts (e.g. at 144827) a high concentration of small droplets is present. In the downdraughts large droplets are present in higher concentrations but the concentration of small drops is lower. The liquid water content (not shown) shows no obvious correlation with vertical velocity.

b. Microphysical processes

As described previously the droplet spectrum in the downdraughts is significantly different from that in the updraughts. The difference is observed through the depth of the cloud suggesting the importance of cloud top processes. Here two processes can occur in addition to those which occur in the interior of the cloud to affect droplet growth. These are entrainment and radiative cooling.

Entrainment of dry air through mixing in an inhomogeneous way would result in fluctuations in droplet concentration but not in the shape of the droplet spectrum. On the other hand homogeneous mixing should result in fluctuations in the position of the peak radius but the concentration should be almost constant. Although the presence of mixing was inferred from profile 2 it was not apparent in profile 3 near 53°55'N. Fluctuations in the droplet spectrum were observed at both locations suggesting that mixing is not the cause of the fluctuations.

Near to cloud top is a region of radiative flux divergence, the cloud radiative layer (CRL). Studies of daytime maritime stratocumulus during JASIN (Slingo et al. 1982b), in which the longwave and shortwave fluxes were measured, indicated that near cloud top the longwave cooling dominates the shortwave heating. Studies of nocturnal stratocumulus (Slingo et al. 1982a) show that the CRL is typically 50 m in depth. The net longwave loss from cloud top is about $50-100 \text{ W m}^{-2}$ with clear skies above, leading to radiative cooling rates of 5 deg C hr^{-1} to 10 deg C hr^{-1} . Water droplet growth under such conditions may be enhanced, as described by Roach (1976), who included an extra term for radiative growth in the droplet growth equation. In a typical roll circulation a parcel may spend a substantial time in the CRL and the radiative effect may be significant. In order to examine the significance of this effect

a numerical model has been used. The model simulations are discussed in section 5.c.

c. Numerical studies of the evolution of the droplet spectrum

A simple Lagrangian parcel model was used to calculate changes in a typical droplet spectrum during ascent and descent of a cloud parcel. The model is described by Ouldrige (1980) who shows that it is able to realistically simulate the mean droplet field in stratocumulus. In the present simulations the model has been extended as described by Caughey et al. (1982b) to include radiative cooling and radiative growth of the droplets. No mixing was included in the model. The nucleus mass was the independent variable and the droplet radii were calculated and held explicitly at each time step as the dependent variable. Activation spectra are usually presented in the form $N = CS^K$, where N is the number density of cloud condensation nuclei active at a supersaturation $S(\%)$, C is the number density active at 1% and C and K are roughly constant. The spectrum specified was with a constant $K = 1.0$ and $N = 1000 \text{ cm}^{-3}$ at $S = 1\%$ and is that given by Ouldrige (1980) as being appropriate for urban air. This should be representative of the airmass having been modified by a long passage over the British Isles. Radiation parameters were taken from the results of Slingo et al. (1982a). A linear profile of \mathcal{R} (the net radiative gain per unit surface area of droplet) from 0 Wm^{-2} at 50 m below cloud top to -50 Wm^{-2} at cloud top was assumed together with a similar linear cooling profile from 0 to 5 deg C hr^{-1} . The parcel trajectory was then chosen to be representative of a roll circulation. The rolls at $53^{\circ}55'N$ were chosen for comparison because (i) no mixing in of drier air was obvious in this area and (ii) data was available at more levels in the cloud for comparison. The parcel trajectory is shown schematically in Fig. 13, the parcel was assumed to ascend vertically from the surface to a height of 200 m and then to overturn following an elliptical path with $a = 500 \text{ m}$ and $b = 200 \text{ m}$ (a and b are the ellipse semimajor and

semiminor axes). This is an approximation to the parcel trajectory in rolls of 2 km updraught spacing and depth 400 m. The entire trajectory was followed at a constant speed W . As shown by Ouldridge (1980) the droplet concentration is dependent upon updraught velocity. It was found that using the nucleus spectrum described earlier a parcel speed of 0.5 ms^{-1} produced droplet concentrations similar to those observed. The parcel speed also determines the time that the parcel spends in the CRL, for $W = 0.5 \text{ ms}^{-1}$ this is about 20 minutes. The magnitude of updraught and downdraught velocities in the cloud sometimes exceeded 0.5 ms^{-1} but this value is representative of most of the cloud.

The results show that the model is able to simulate a substantial change in the droplet spectrum following the parcel trajectory when radiative growth is included in the model. Figs. 14(a) - 14(d) show comparisons of observed and model spectra 150 m above the sea surface and Figs. 15(a) - 15(d) show similar data at 300 m. The model spectra have been plotted in the same size categories as are used for the ASSP measurements to allow direct comparison with the measurements (the size ranges are given in Table 1). The observed spectra are averages of spectra obtained in updraught/downdraught regions over a five minute segment of data around $53^{\circ}55'N$. The model spectra show less dispersion, particularly in the updraught, but this is not surprising since the model includes no mixing. The model spectra in the downdraught show that the droplet concentration predicted by the model is lower than that in the updraught (as was observed) and that there are significantly more larger droplets (radius $>8 \mu\text{m}$). The model was also run without radiative cooling and the model spectra obtained in the downdraught at 150 m and 300 m height are shown by the dashed spectra in Figs. 14(d) and 15(d). Without radiative cooling few drops grow to a radius of greater than $8 \mu\text{m}$ and the concentration in the downdraught is not reduced in the same manner. These results show that, within the simple framework of the model, radiative cooling can result in drops growing to the sizes observed and can also result in a marked reduction in droplet concentration in the downdraught. This

is because as the air descends through the CRL, the drops experience an undersaturation. The smaller drops evaporate in this subsaturated downdraught but the larger drops continue to grow since they are cooled below the ambient air temperature by radiative loss. It should be noted that in the downdraught in the model there are a small number of drops present at sizes below those which would be detected by the ASSP (of radius $<3.3\mu\text{m}$). The concentrations given in the diagrams (Figs. 14 and 15) are for drops of radius greater than $3.3\mu\text{m}$ in both the observed and simulated spectra. The presence of these smaller droplets in the downdraught implies that the model and observed droplet concentrations quoted are lower than they really are, however this does not significantly influence the conclusions. The model is not designed to accurately reproduce the observed spectra as a cloud parcel may have been cycled repeatedly and undergone turbulent mixing within the cloud, both of which can modify the droplet spectrum. The model results indicate that radiative growth in the CRL is capable of producing significant changes in the droplet spectrum, which are consistent with those observed. These results lend support to the hypothesis that radiative cooling in the CRL is primarily responsible for the significant droplet spectrum variations observed in the cloud during the level runs.

6. CONCLUDING REMARKS

The data presented illustrate the microphysical and dynamical structure of the cloudy boundary layer. The detailed microphysical measurements suggest that in some areas of the cloud entrainment was occurring and that in other areas it was not. Entrainment occurred when the cloud top inversion was weakest and the data suggests that its effects were consistent with the inhomogeneous model. In one area of cloud large droplets of radius greater than $20\mu\text{m}$ were observed and it is suggested that they were due to coalescence.

The most striking feature of the microphysical data is the presence of significant variations in the droplet spectrum observed during the level runs resulting from the dynamical structure of the boundary layer. Horizontal roll vortices were occurring within the cloud and the microphysical structure in the roll updraughts were very different to those in the downdraughts. It is suggested that radiative cooling in the CRL is primarily responsible for this variation and this conclusion is supported by results from a simple Lagrangian model. The rolls observed in this study are not as well defined as those observed previously by other workers due to the presence of significant "kilometer scale turbulence". The study shows evidence that the microphysical processes occurring in the boundary layer depend in a fundamental way on the dynamical processes that determine the structure of the circulation.

Table 1 ASSP channel sizes

ASSP channel (Range 1)	Channel mid point radius (μm)
1	3.7
2	4.8
3	6.0
4	7.4
5	8.8
6	10.2
7	11.6
8	13.1
9	14.5
10	16.0
11	17.5
12	19.0
13	20.5
14	21.9
15	23.4

References

- Axford, D.N. 1971 Spectral analysis of an aircraft observation of gravity waves.
Quart. J. R. Met. Soc., 97, 313-321.
- Caughey, S.J. and 1979 Some aspects of the turbulence
Palmer, S.G. structure through the depth of the
convective boundary layer.
Ibid, 105, 811-827.
- Caughey, S.J., 1982a A field study of nocturnal stratocumulus;
Crease, B.A. and II. Turbulence structure and entrainment.
Roach, W.T. Ibid, 108, 125-144.
- Caughey, S.J., 1982b Simultaneous measurements of the
Kitchen, M. and turbulent and microphysical structure
Roach, W.T. of nocturnal stratocumulus cloud.
Quart. J. R. Met. Soc., submitted to
- Cornford, S.G. 1966 Stratocumulus - a review of some
physical aspects.
Met. Mag., 95, 292-304.
- Coulman, C.E. 1978 Convection in stratiform cloud.
J. Rech. Atmos., 12, 21-33.

- Crabtree, J. and Marsh, A.R.W. 1981 Instrumentation of the Hercules aircraft of the Meteorological Research Flight.
Unpublished Met. Office Met O 14
T.D.N. No. 127.
- Fisher, B.E.A. 1981 Acid rain and the long range transport of air pollutants.
Weather, 36, 367-369.
- Frith, R. 1951 The size of cloud particles in stratocumulus cloud.
Quart. J. R. Met. Soc., 77, 441-444.
- James, D.G. 1959 Observations from aircraft of temperatures and humidities near stratocumulus clouds.
Ibid, 85, 120-130.
- Johnson, D.A. 1979 A study of the Johnson-Williams liquid water content meter as fitted to the M.R.F. Hercules.
Unpublished Met. Office Met O 15
Internal Report No. 22.
- Knollenberg, R.G. 1970 The optical array: an alternative to scattering or extinction for airborne particle size determination.
J. Appl. Met., 9, 86-103.

- Knollenberg, R.G. 1976 Three new instruments for cloud physics measurements.
Reprint Vol. Int. Conf. Cloud Physics, Boulder, Colorado, 554-561.
- Konrad, T.G. 1968 The alignment of clear air convective cells.
Proc. Int. Conf. Cloud Physics, Toronto, Canada, 539-543.
- Kuettner, J.P. 1971 Cloud bands in the earth's atmosphere: observations and theory.
Tellus, 23, 404-425.
- Latham, J. and 1977 Laboratory studies of the effects of
Reed, R.L. mixing on the evolution of cloud droplet spectra.
Quart. J. R. Met. Soc., 103, 297-306.
- LeMone, M.A. 1973 The structure and dynamics of horizontal roll vortices in the planetary boundary layer.
J. Atmos. Sci., 30, 1077-1091.
- LeMone, M.A. 1976 Modulation of turbulence energy by longitudinal rolls in an unstable boundary layer.
Ibid, 33, 1308-1320.

- Mason, P.J. and Sykes, R.I. 1980 A two-dimensional numerical study of horizontal roll vortices in the neutral atmospheric boundary layer. Quart. J. R. Met. Soc., 106, 357-366.
- Mason, P.J. and Sykes, R.I. 1982 A two-dimensional numerical study of horizontal roll vortices in an inversion capped planetary boundary layer. Ibid, 108, 801-823.
- Nicholls, S. 1978 Measurements of turbulence by an instrumented aircraft in a convective atmospheric boundary layer over the sea. Ibid, 104, 653-676.
- Ouldrige, M. 1980 A Lagrangian approach to the simulation of the condensation process. Proc. Int. Conf. Cloud Physics, Clermont-Ferrand, 337-340.
- Ouldrige, M. 1982a An introduction and guide to the PMS 2-D optical array spectrometer system. Unpublished Met. Office Met O 15 Internal Report No. 39.
- Ouldrige, M. 1982b An introduction and guide to the Johnson-Williams liquid water content meter. Unpublished Met. Office Met O 15 Internal Report No. 41.

- Paltridge, G.W. 1974 Infrared emissivity, shortwave albedo and the microphysics of stratiform water clouds.
J. Geophys. Res., 79, 4053-4058.
- Platt, C.M.R. 1976 Infrared absorption and liquid water content in stratocumulus clouds.
Quart. J. R. Met. Soc., 102, 553-561.
- Roach, W.T. 1976 On the effect of radiative exchange on the growth by condensation of a cloud or fog droplet.
Ibid, 102, 361-372.
- Roach, W.T. 1977 Performance assessment of the Knollenberg Axially Scattering Spectrometer, model ASSP-100.
Unpublished Met. Office Met O 15
Internal Report No. 8.
- Roach, W.T., Brown, R., 1982 A field study of nocturnal stratocumulus
Caughey, S.J., I. Mean structure and budgets.
Crease, B.A. and Quart. J. R. Met. Soc., 108, 103-123.
Slingo, A.
- Ryder, P. 1976 The measurement of cloud droplet spectra.
Reprint Vol. Int. Conf. Cloud Physics,
Boulder, Colorado, 576-580.
- Slingo, A., Brown, R. 1982a A field study of nocturnal stratocumulus;
and Wrench, C.L. III. High resolution radiative and microphysical observations.
Quart. J. R. Met. Soc., 108, 145-165.

Slingo, A., Nicholls, S. 1982b Aircraft observations of marine
and Schmetz, J. stratocumulus during JASIN.

Ibid, 108, 833-856.

Stewart, J.B. 1964 Precipitation from layer cloud.

Ibid, 90, 287-297.

Figure captions

- Figure 1 Synoptic chart for 1200 GMT, 28 January 1981. The positions of the aircraft runs are shown by the solid line off the east coast of England.
- Figure 2 VHRR visible image from NOAA-6, taken at 0923 GMT, 28 January 1981. Registration error is about 40 km over the UK. Photograph by courtesy of the University of Dundee.
- Figure 3 Cross-section of the cloud layer. The solid line shows isotherms in degC, the dashed line shows the aircraft level run and profile positions. Cloud base is indicated, cloud top coincides with the base of the inversion.
- Figure 4 Profiles of (a) temperature, (b) liquid water content, (c) droplet concentration and (d) droplet mean volume radius obtained during profile 2. The cloud layer is indicated by the arrow, the solid line in (b) is the adiabatic liquid water profile.
- Figure 5 Profile of droplet concentration reconstructed from ASSP and PMS 2D data. The isopleths show the concentration of droplets (in cm^{-3}) larger than a given radius, e.g. at 400 m height the concentration of droplets larger than $10 \mu\text{m}$ radius is 10 cm^{-3} . The maximum dropsizes observed is indicated by the dashed line.
- Figure 6 As for figure 4, but during profile 3.

- Figure 7 Time series of vertical velocity fluctuation (a) in cloud from run 7 at 295 m and (b) above cloud from run 6 at 480 m. The spatial scale is indicated.
- Figure 8 Power spectra of vertical velocity fluctuation (a) above cloud from run 6 at 480 m, (b) in cloud from run 7 at 295 m and (c) in cloud from run 5 at 150 m.
- Figure 9 Vertical profile of horizontal wind components measured during profile 2. The cloud layer is indicated by the arrow.
- Figure 10 Variation of characteristic wavelength for the vertical velocity fluctuations $(\lambda_m)_w$ with height in and above the cloud layer. The estimates of $(\lambda_m)_w$ are plotted as plus and minus one spectral estimate.
- Figure 11 Time series of (a) droplet mean volume radius, (b) droplet concentration and (c) vertical velocity fluctuation from run 4 at 175 m. The spatial scale is indicated.
- Figure 12 Time series of (a) droplet concentration, (b) vertical velocity fluctuation and (c) drop-size spectra (where contours of droplet concentration in each ASSP channel are plotted) obtained during run 4 at 175 m. The spatial scale is indicated.
- Figure 13 Parcel trajectory specified for model simulation. The specified profiles of net radiative gain (\mathcal{R}) and radiative cooling rate (H) are also shown.

Figure 14 Observed and model droplet spectra obtained at 150 m,
(a) observed updraught, (b) model updraught, (c) observed
downdraught and (d) model downdraught (the dashed spectra
is produced when radiative growth is omitted in the model).

Figure 15 As for figure 14 but spectra obtained at 300 m.

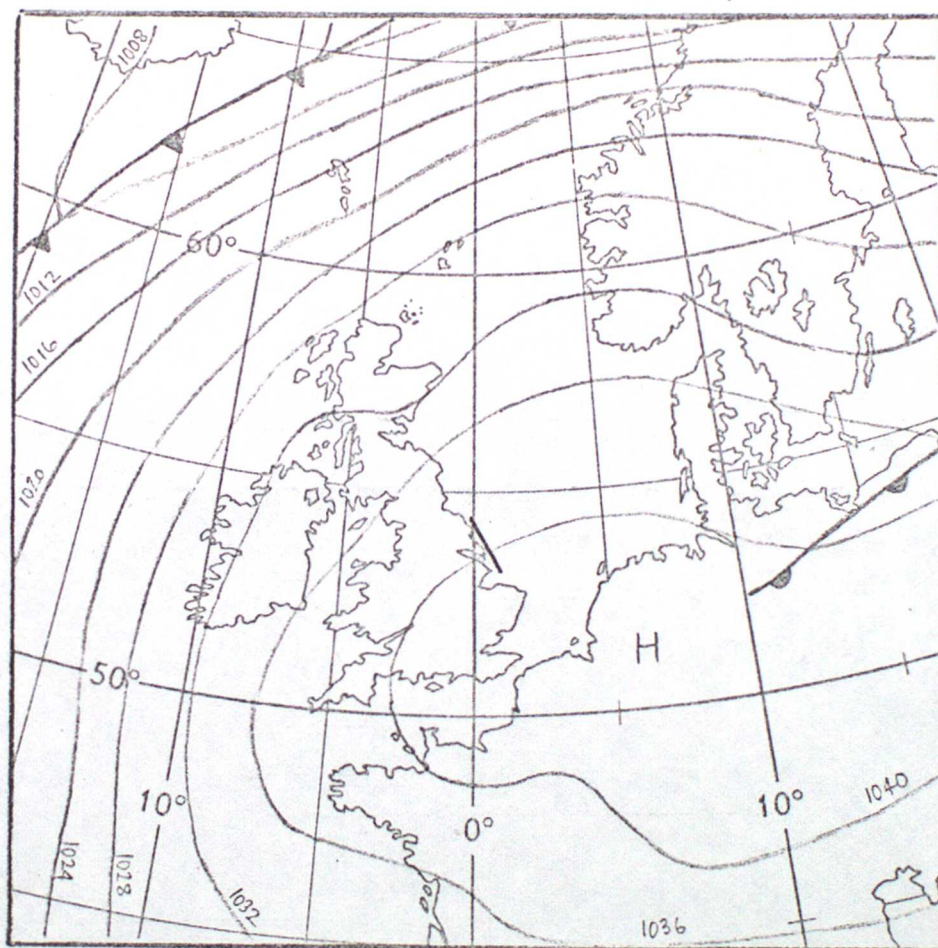


FIG. 1



FIG. 2

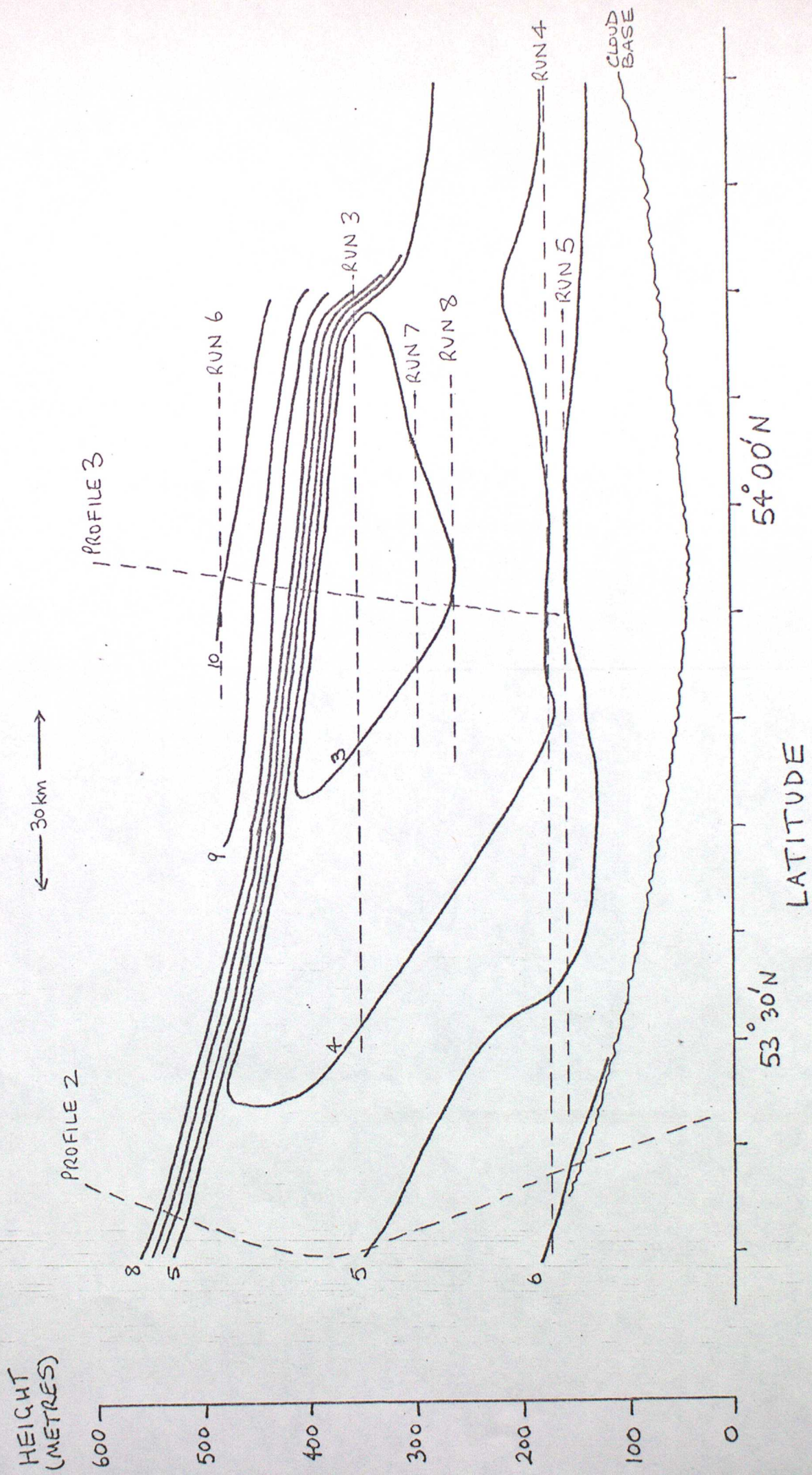


FIG. 3

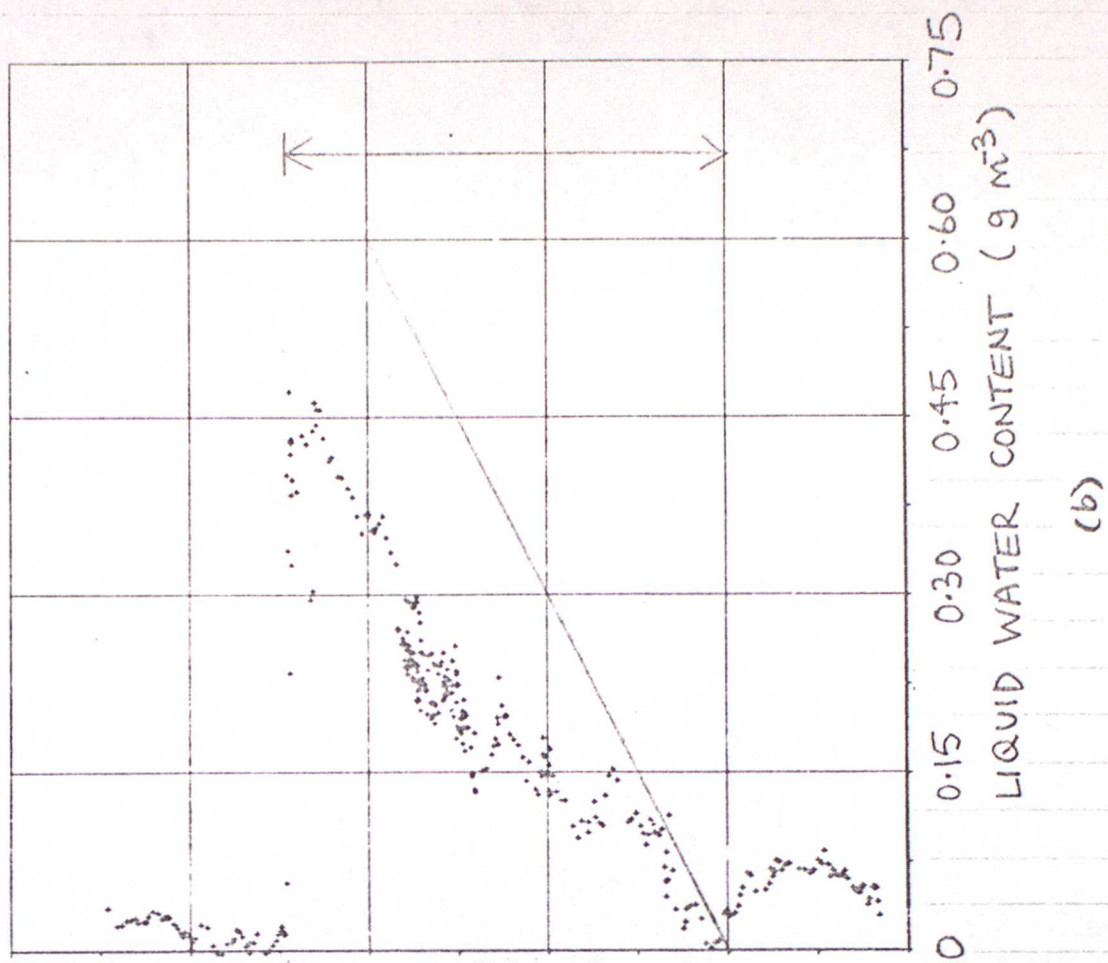
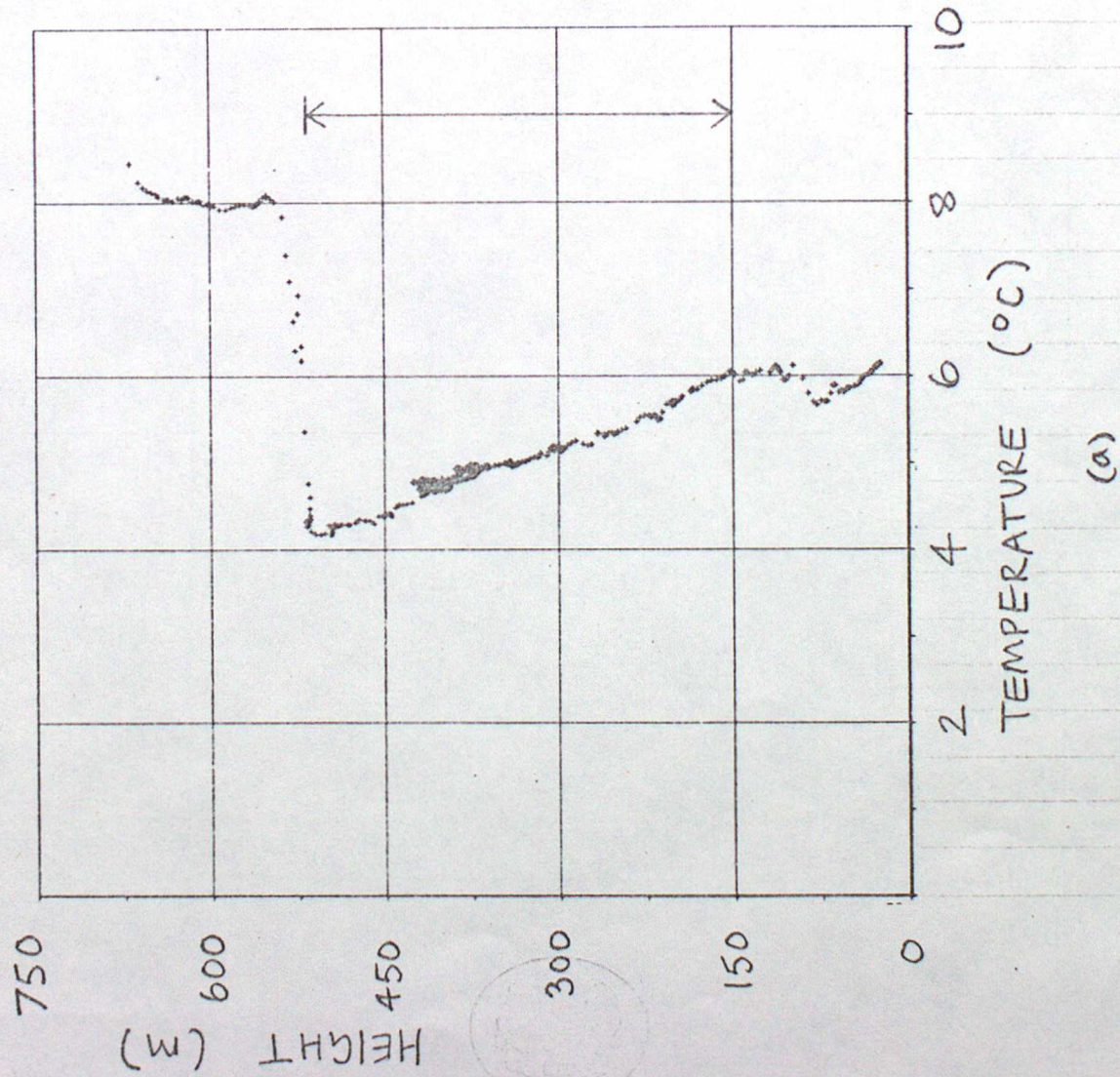


FIG. 4

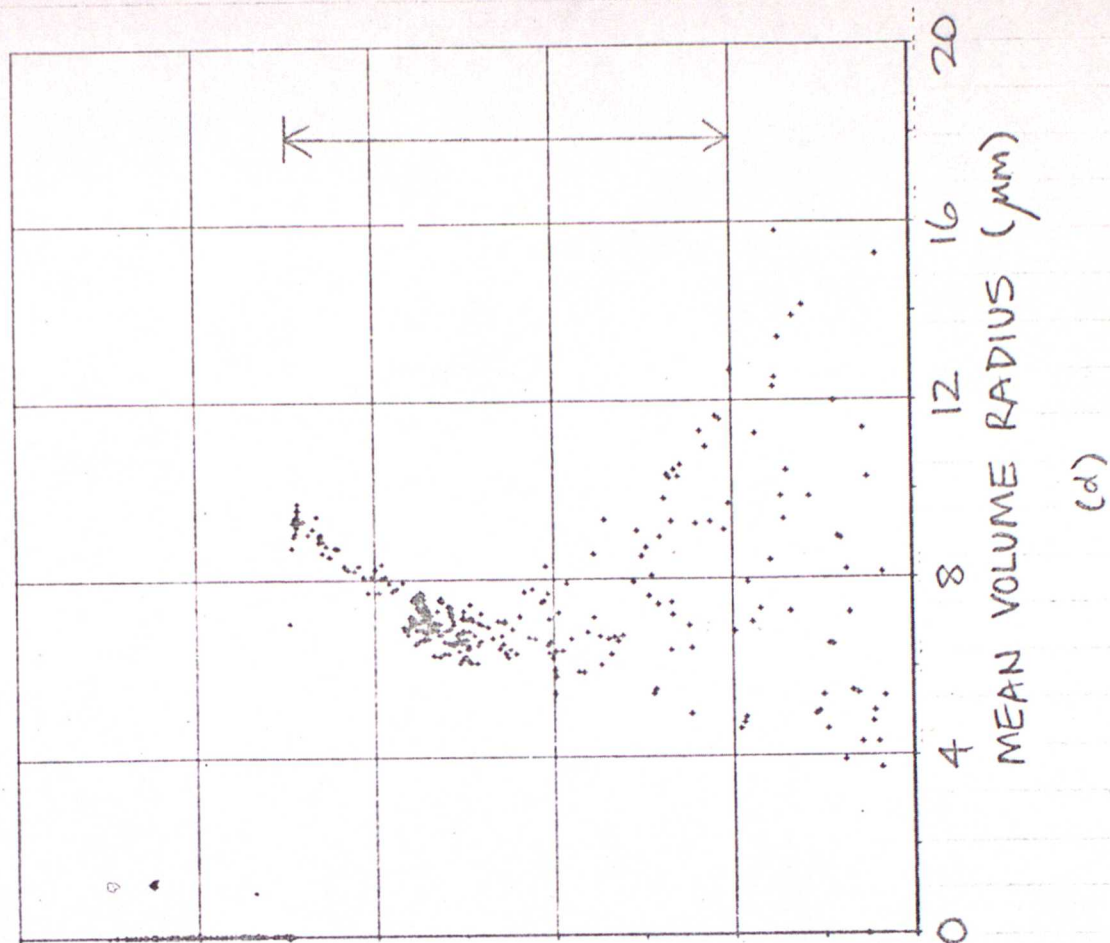
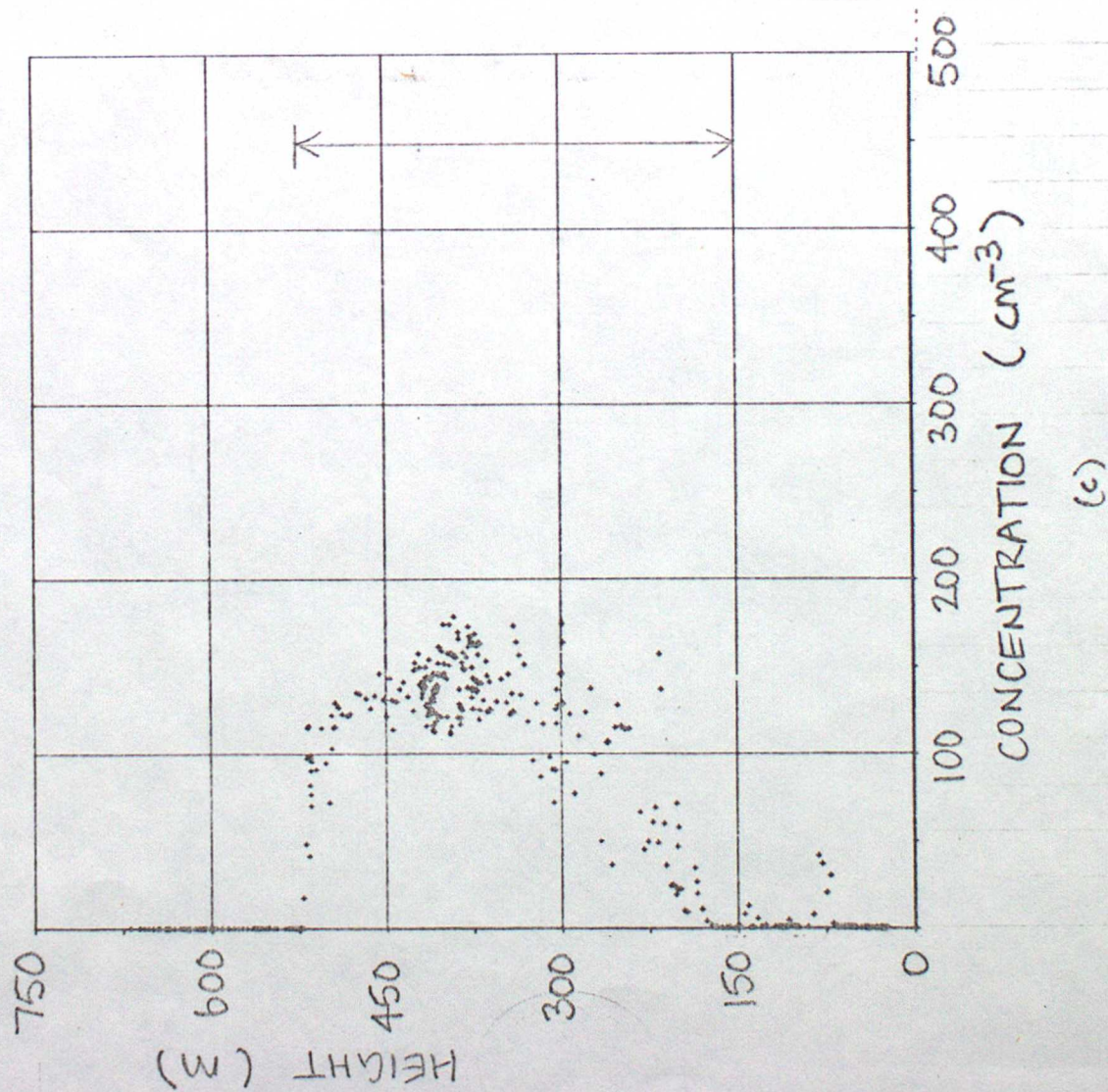


FIG. 4

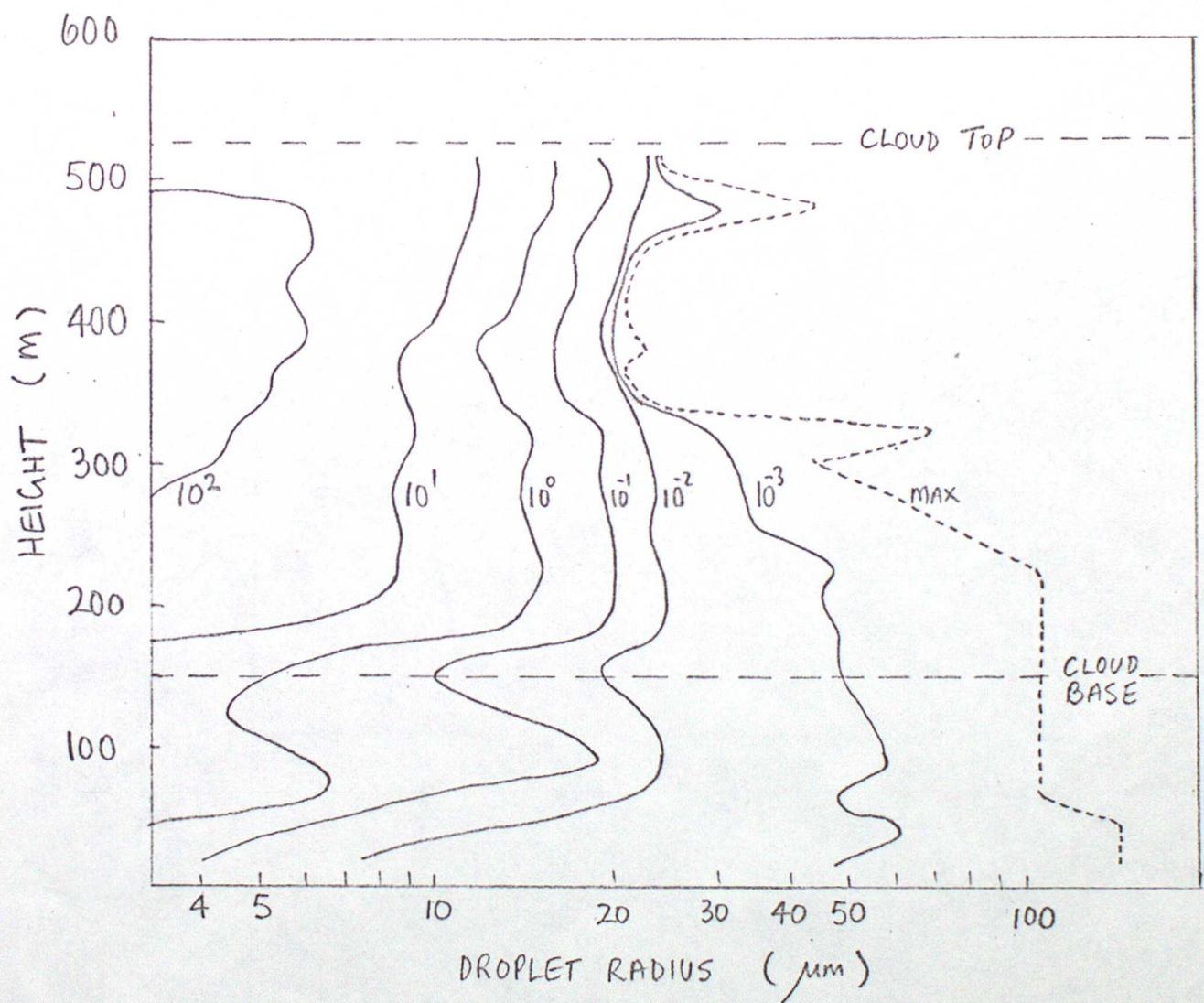


FIG. 5

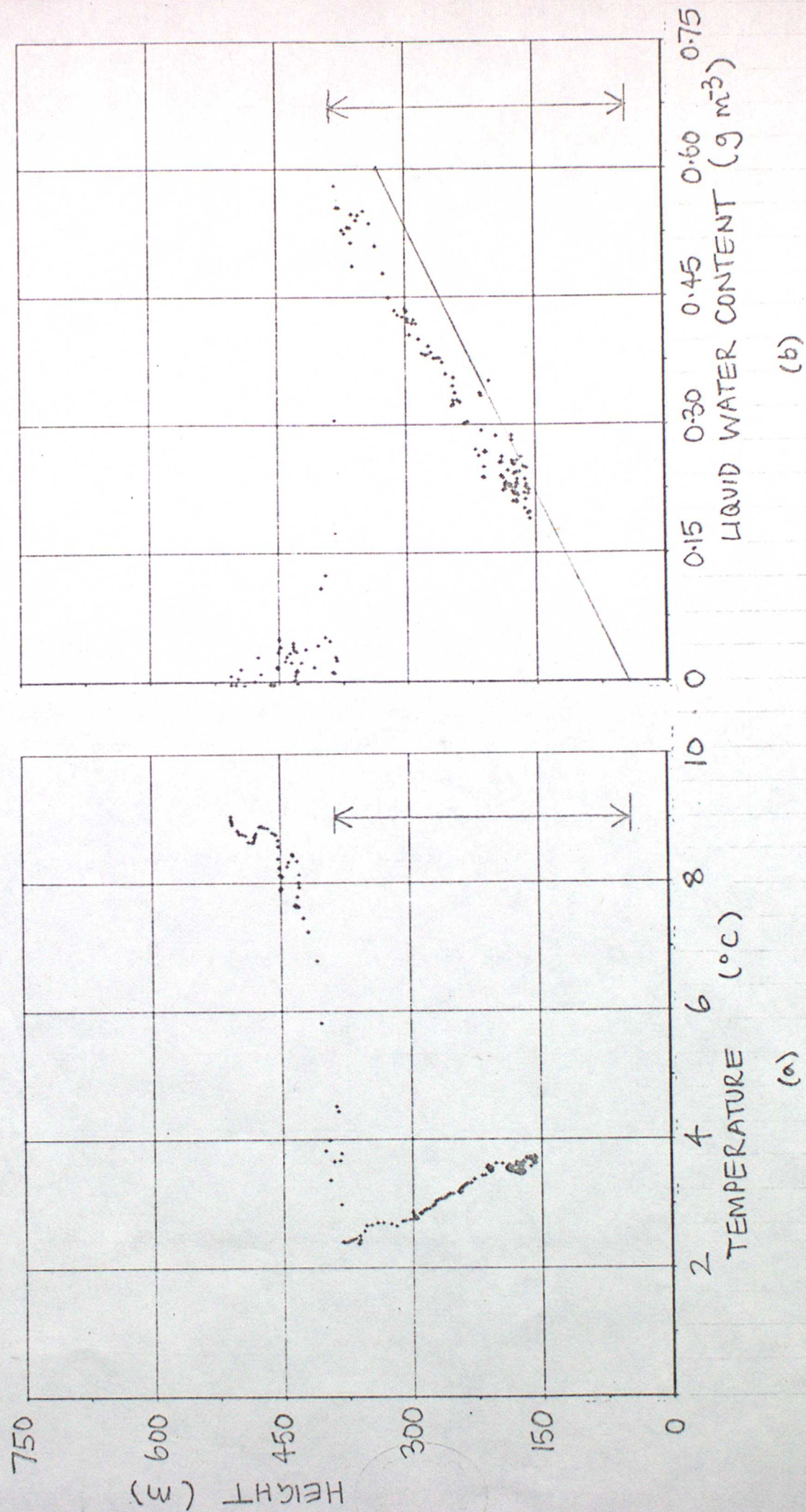
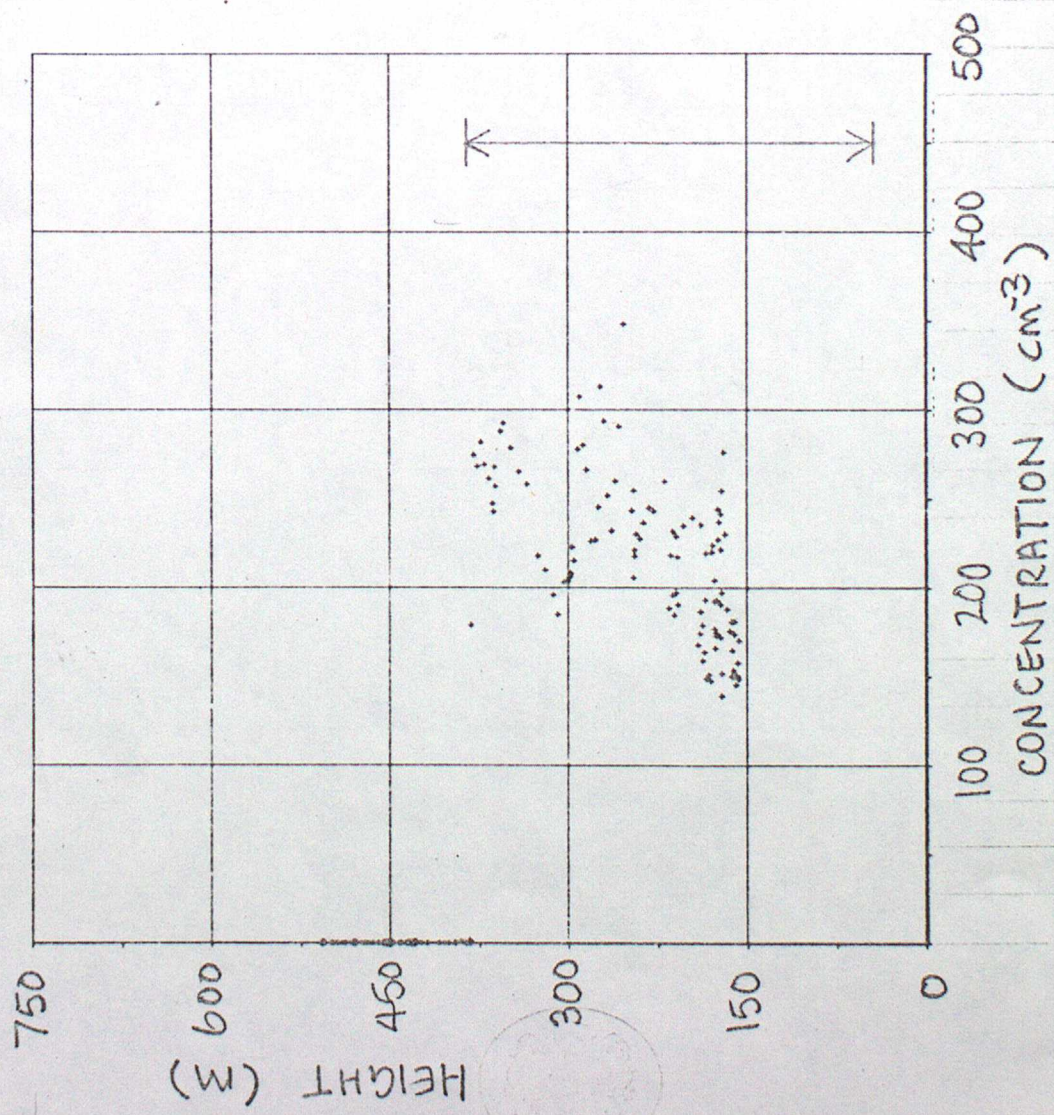
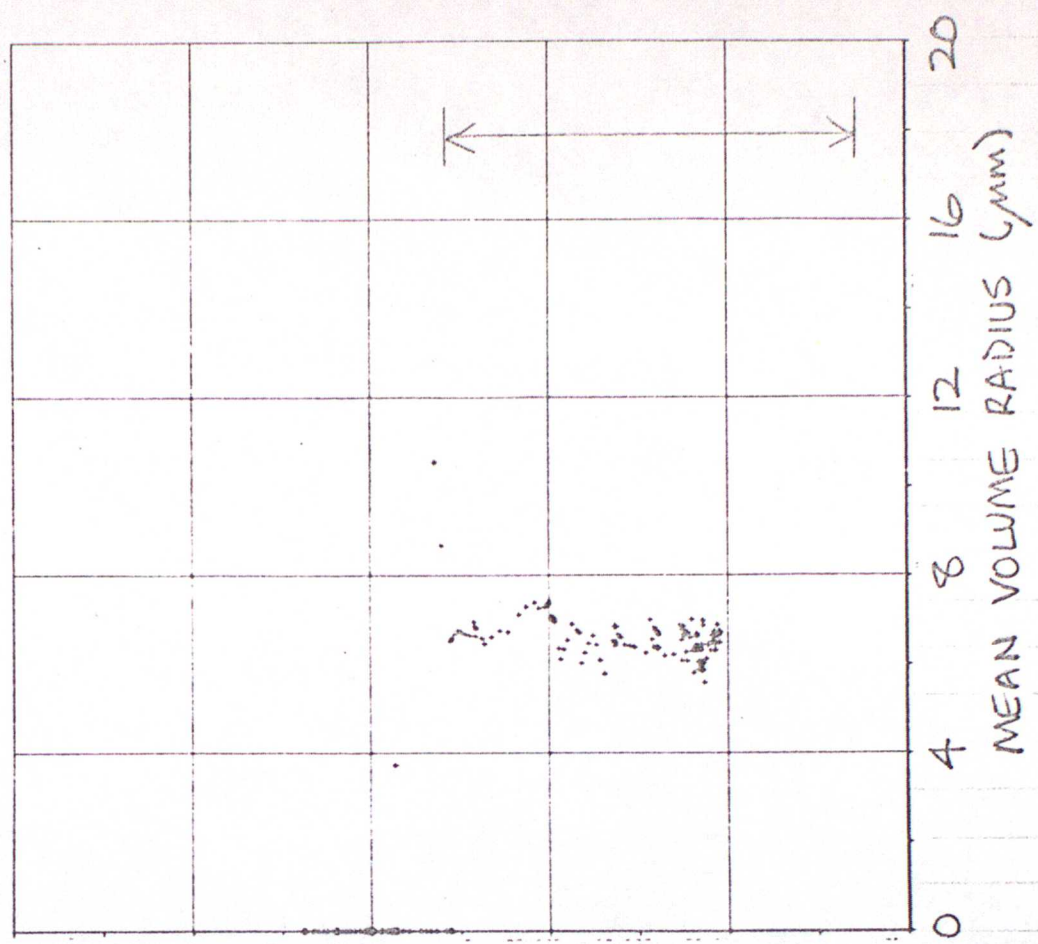


FIG. 6

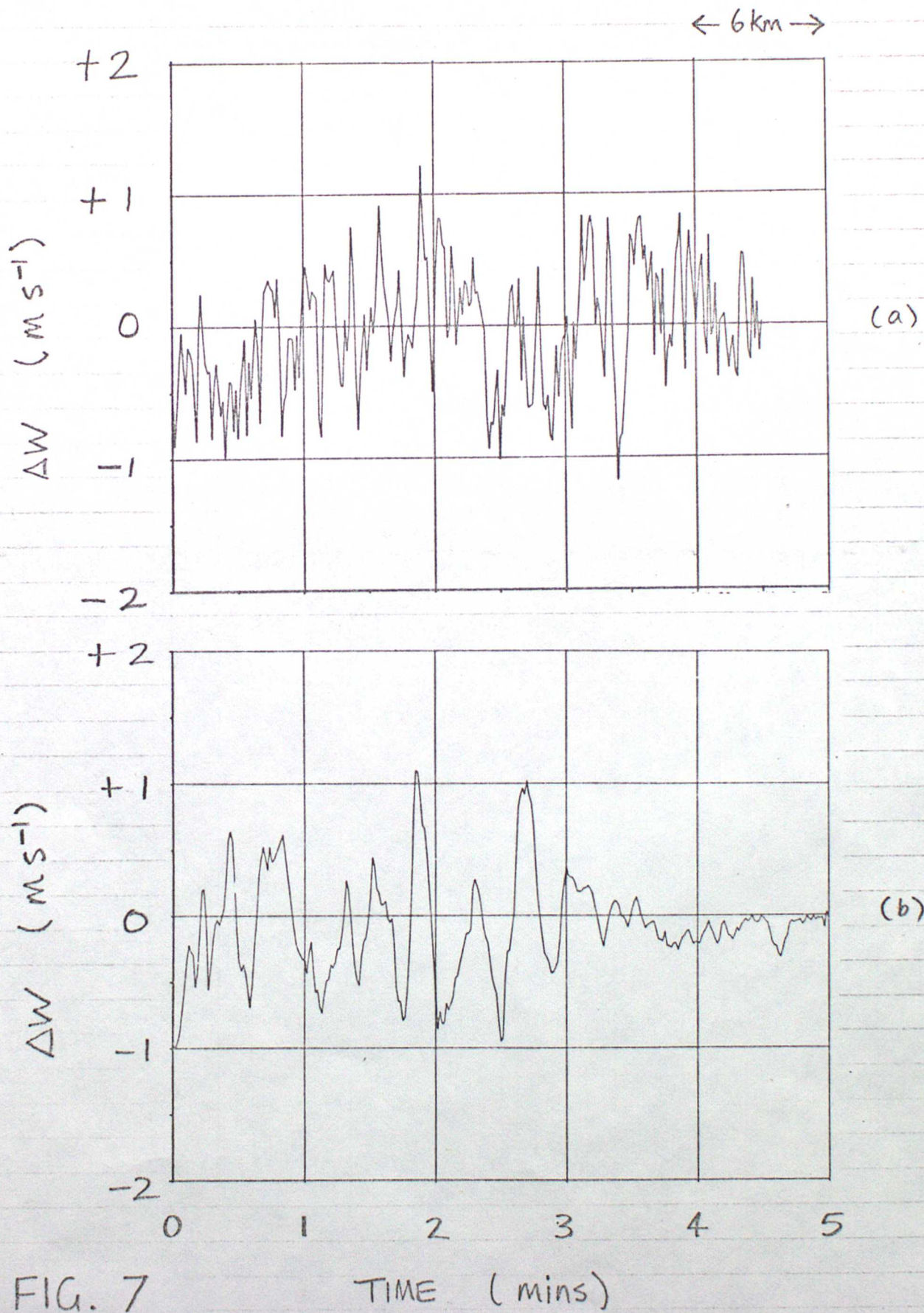


(c)

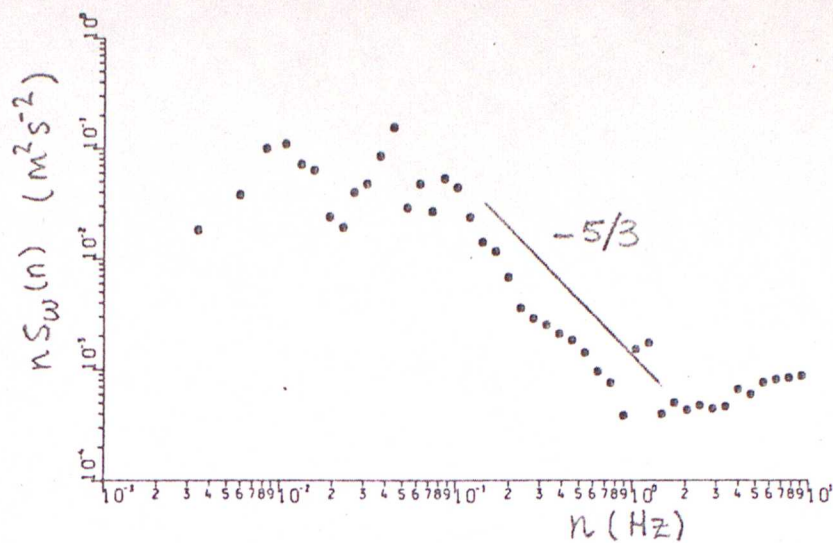


(d)

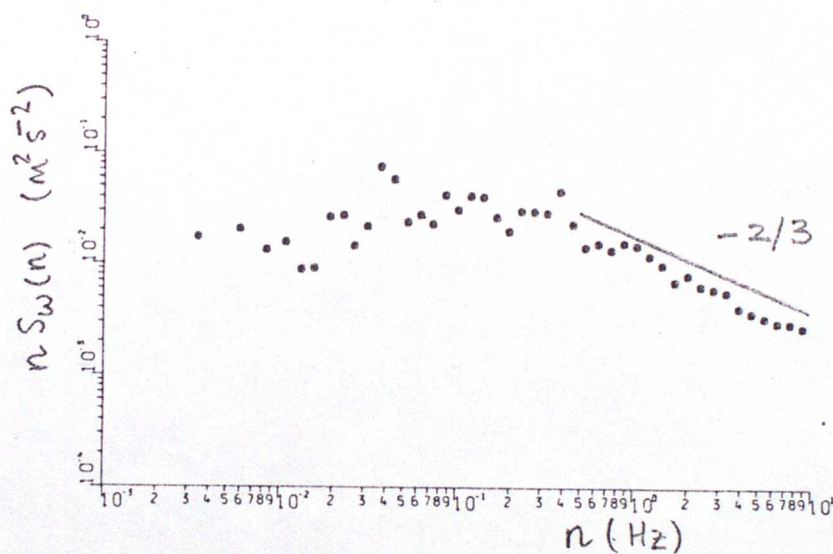
FIG. 6



(a)



(b)



(c)

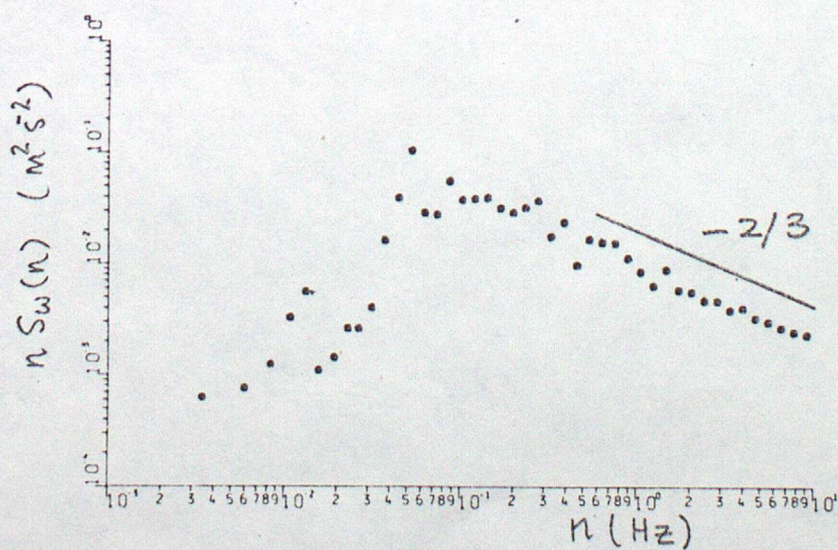


FIG. 8

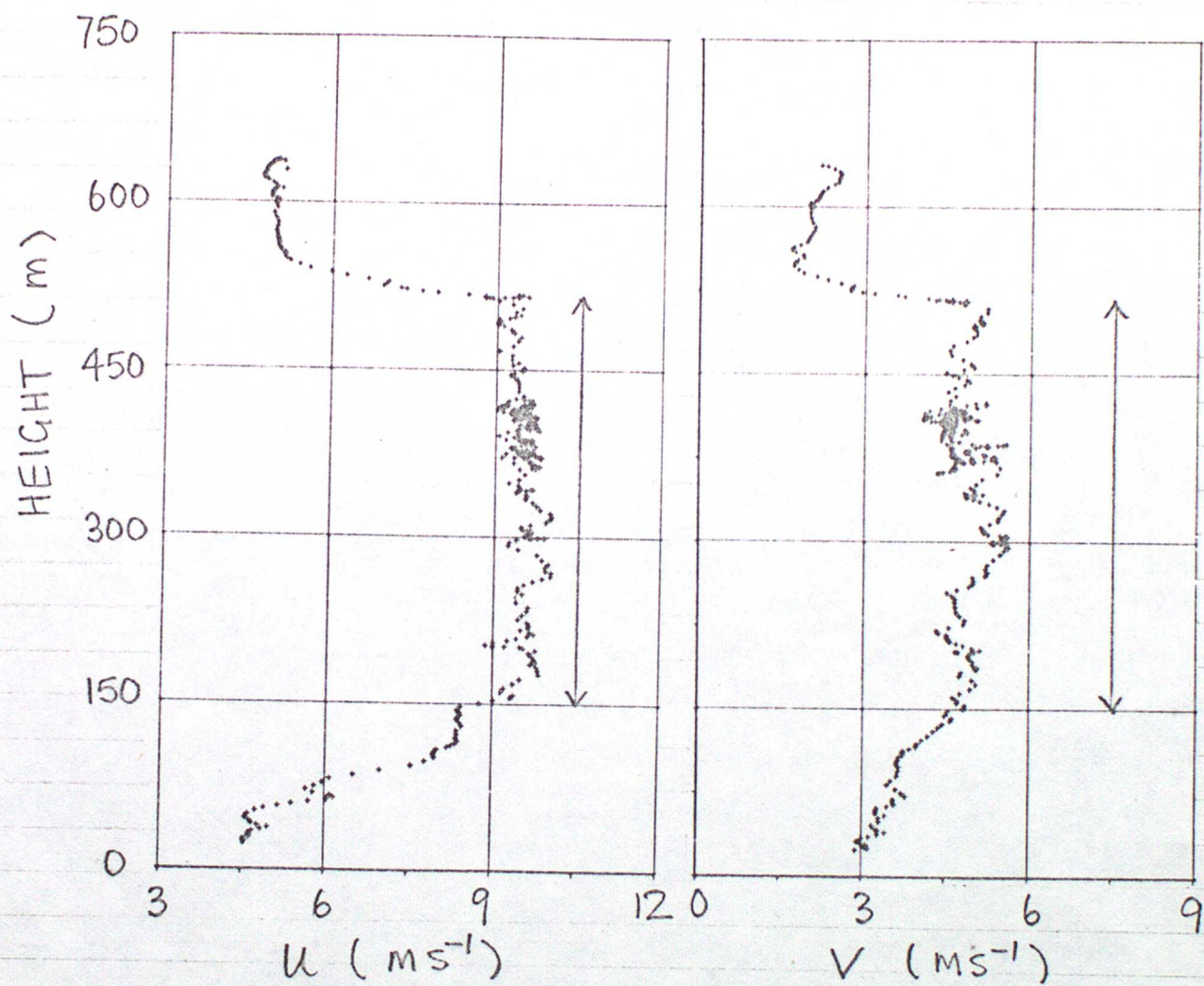


FIG. 9

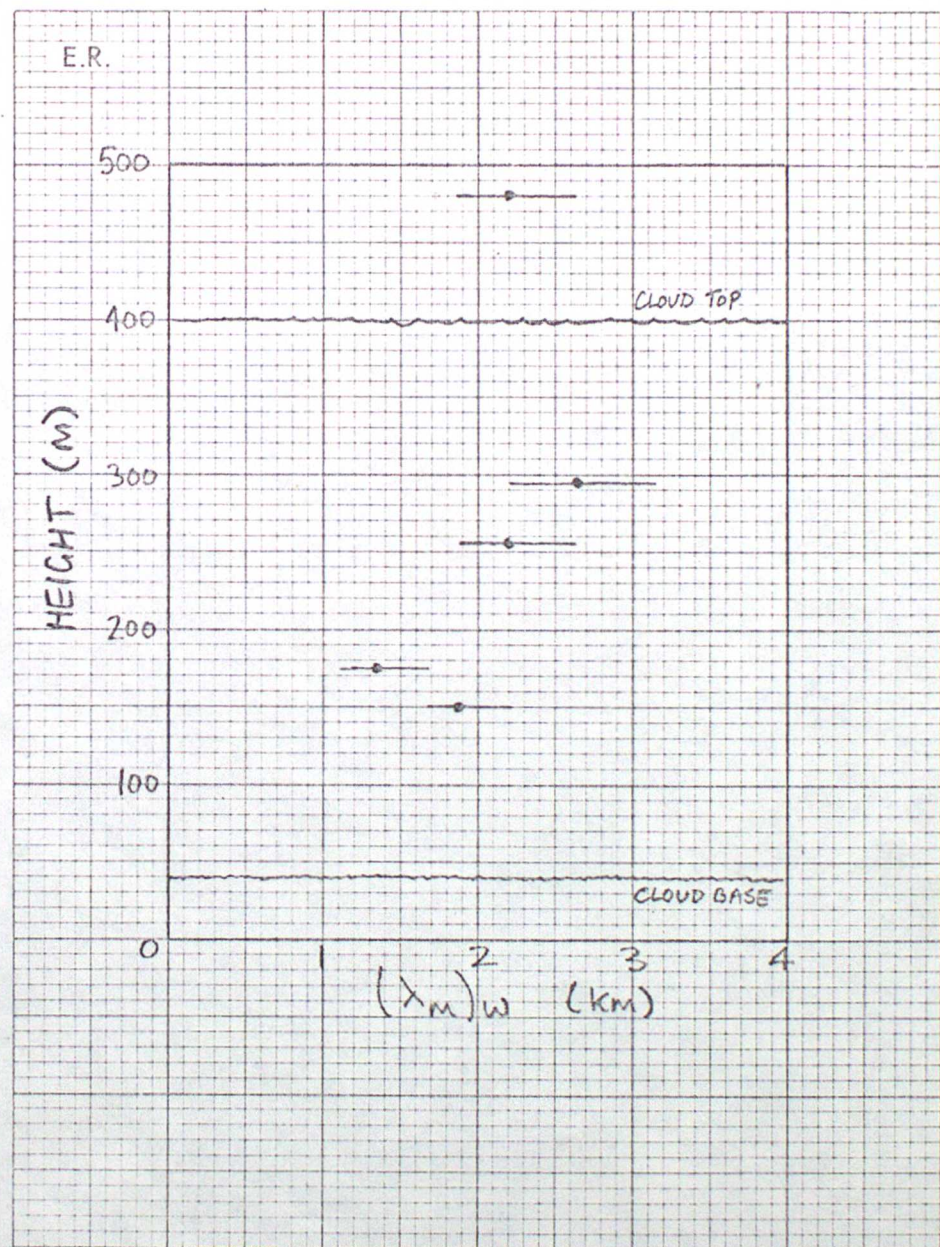


FIG. 10

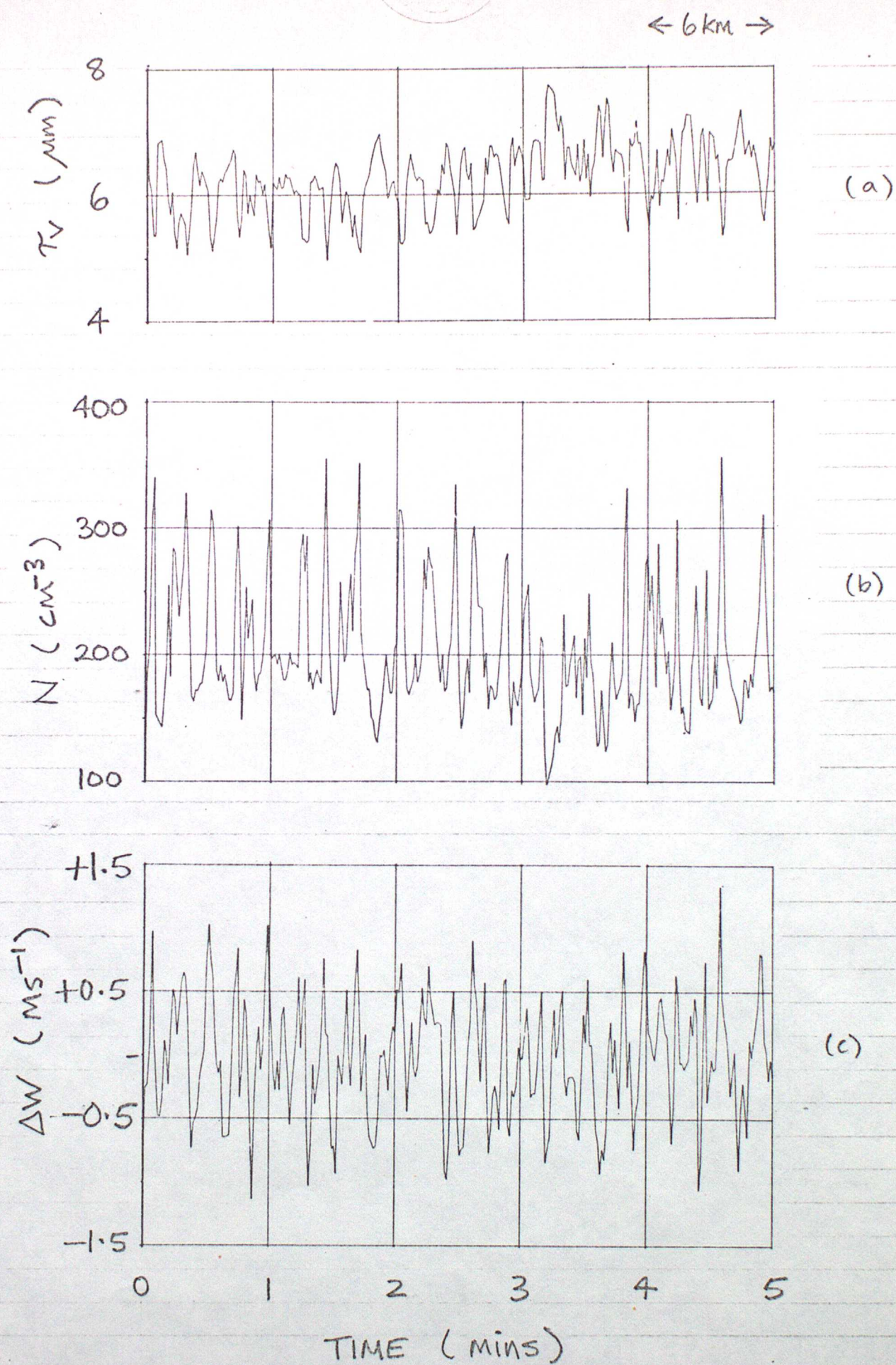
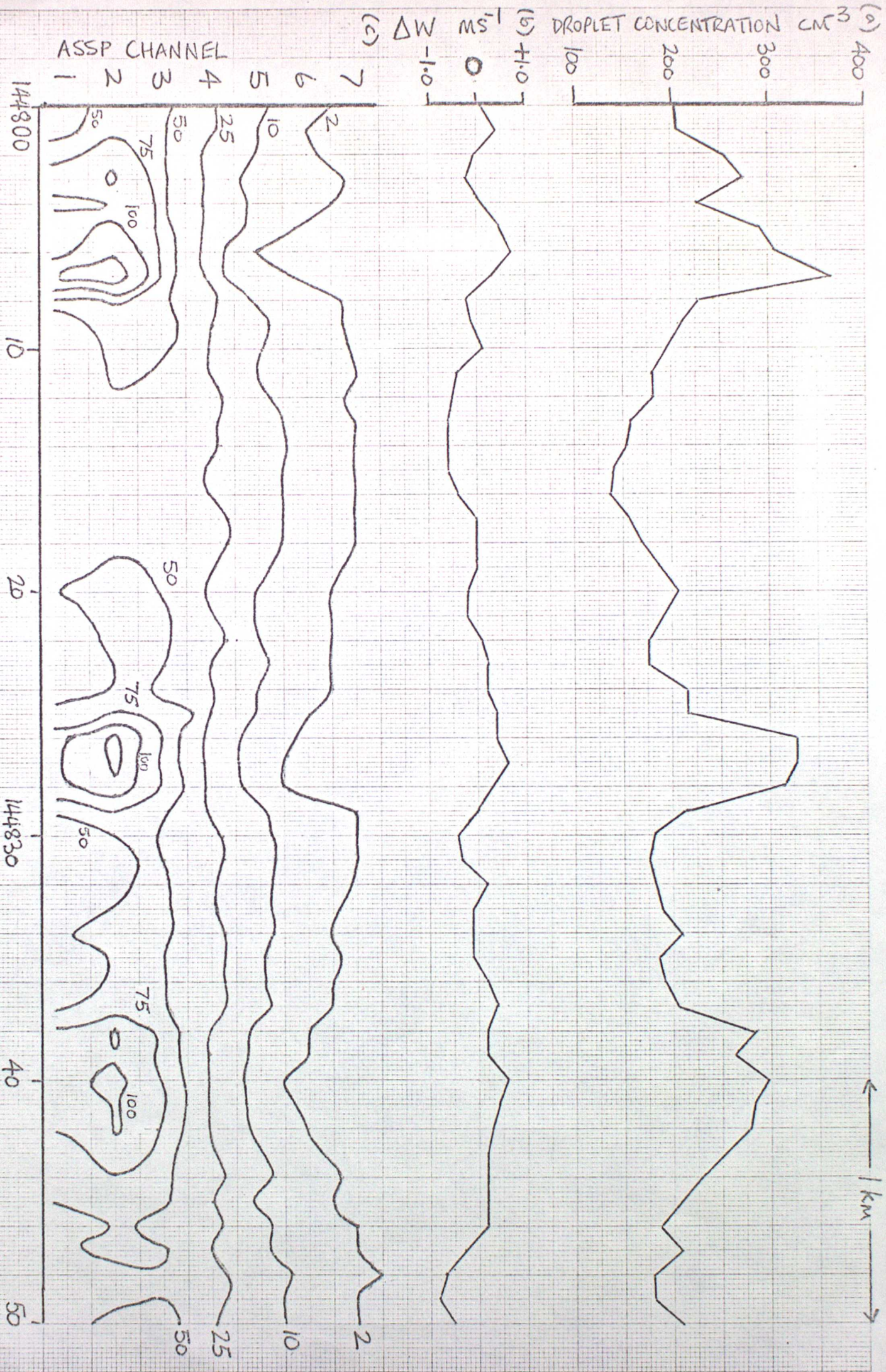


FIG. 11

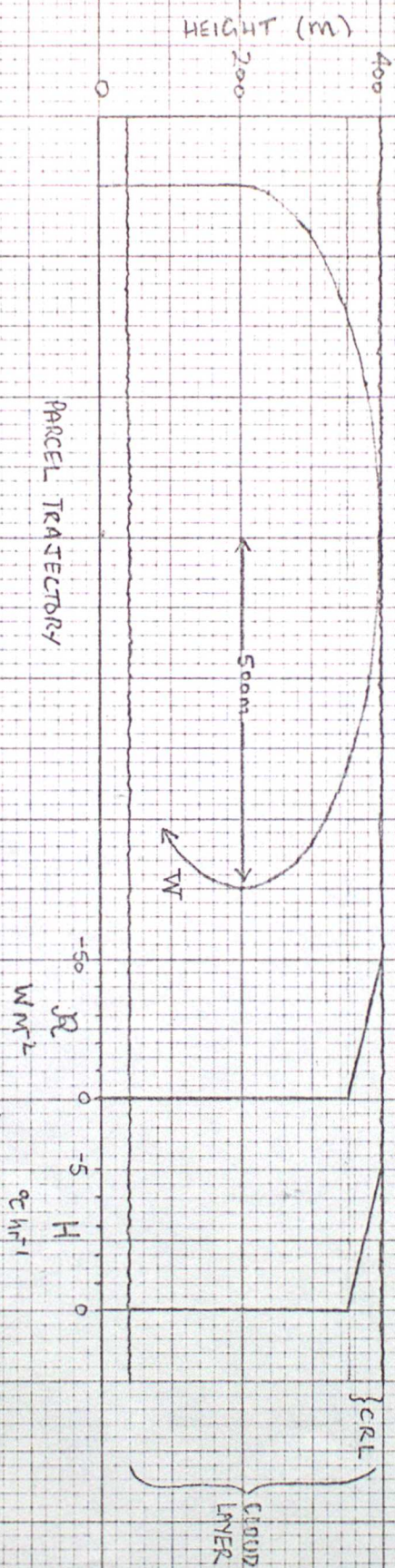
FIG. 12

TIME (GMT)



E.R.

FIG. 13



DROPLET SPECTRA AT 150 m

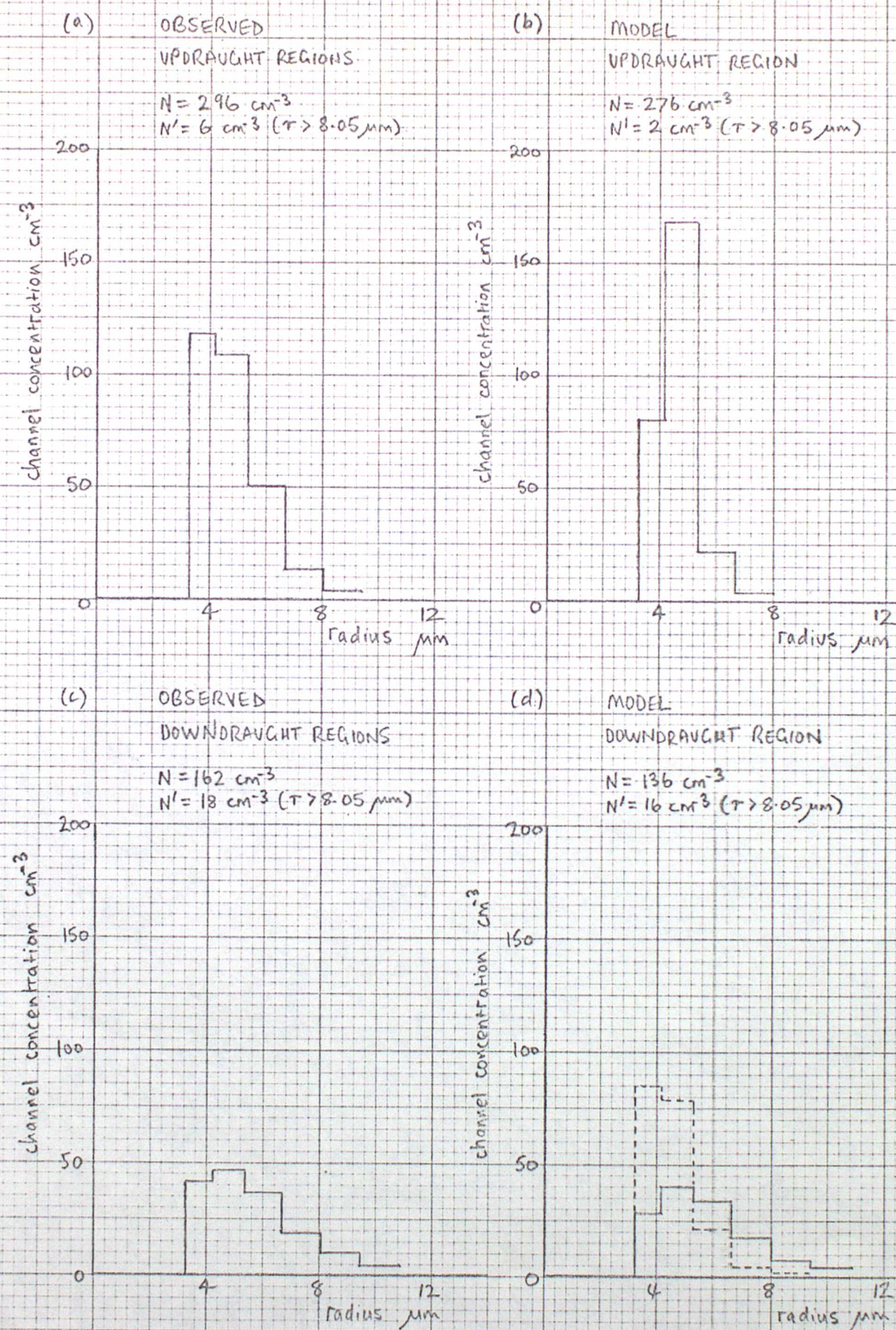


FIG. 14

DROPLET SPECTRA AT 300 m

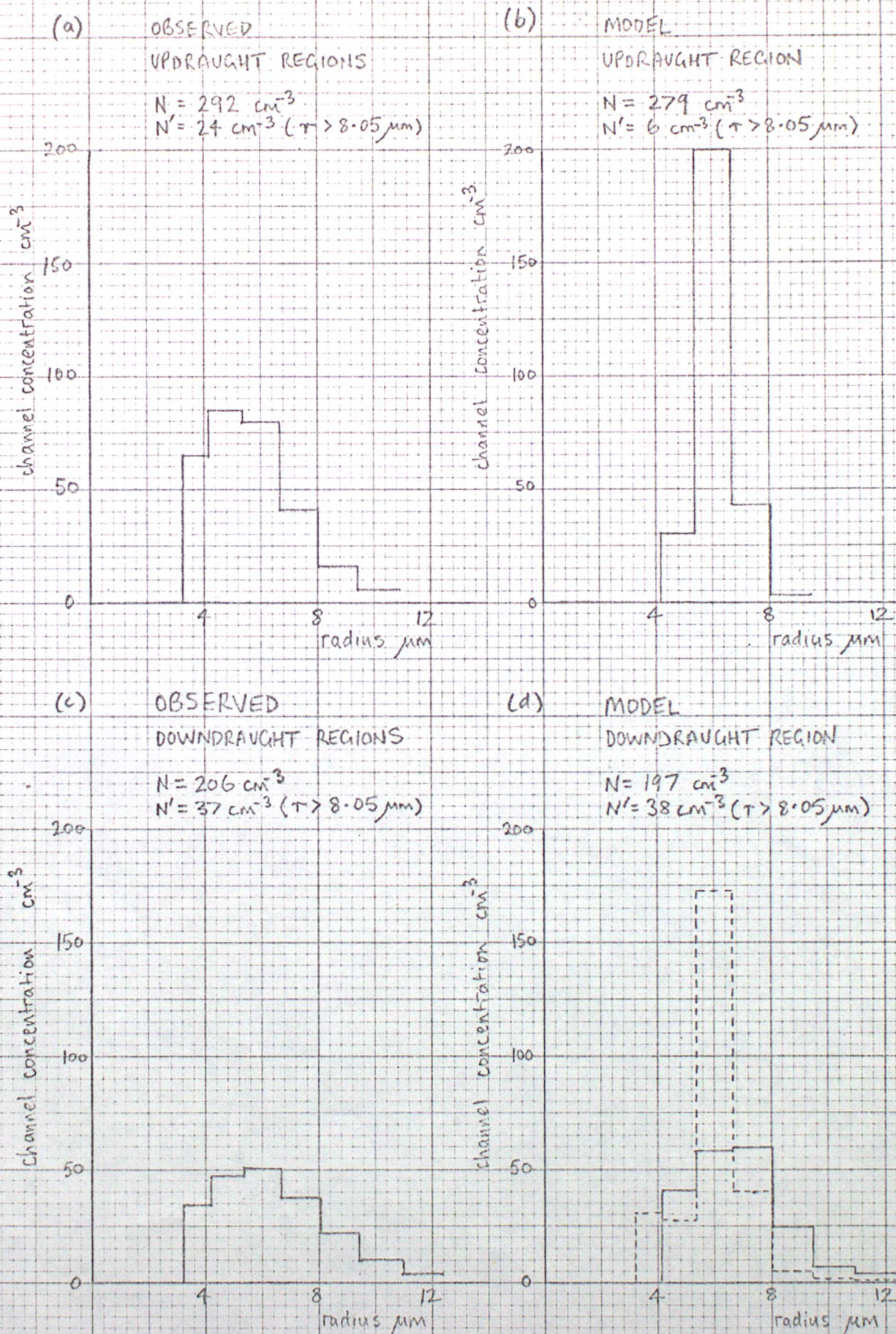


FIG. 15